EurJIC
European Journal of Inorganic Chemistry
ChemPubSoc Europe

DOI:10.1002/ejic.201402224

Heterobinuclear Zn–Ln and Ni–Ln Complexes with Schiff-Base and Carbacylamidophosphate Ligands: Synthesis, Crystal Structures, and Catalytic Activity

Oleksiy V. Amirkhanov,*[a] Olesia V. Moroz,[a]
Kateryna O. Znovjyak,[a] Tetiana Yu. Sliva,[a] Larysa V. Penkova,[a]
Tetyana Yushchenko,[b] Lukasz Szyrwiel,[c] Irina S. Konovalova,[d]
Viktoriya V. Dyakonenko,[d] Oleg V. Shishkin,[d,e] and
Vladimir M. Amirkhanov*[a]

Keywords: Heterometallic complexes / Kinetics / Lanthanides / N,O-ligands / Structure elucidation

The reaction of Salen-like Zn^{II} and Ni^{II} precursors with carbacylamidophosphate lanthanide moieties yields six new types of 3d–4f compounds. The complexes were characterized by means of ^{1}H, ^{31}P NMR and IR spectroscopy, elemental analysis, ESI mass spectrometry, and X-ray diffraction analysis. Depending on the Schiff base ligands, the Ni^{II} ion adopts either a square-planar or an octahedral geometry, whereas the Zn^{II} ion has a tetragonal-pyramidal geometry. The coordination number of lanthanides is nine or ten. Hydrolytic activities of some heterobimetallic Zn–Ln and Ni–Ln coordination compounds in the reaction of intramolecular hydrolytic degradation of the 2-(hydroxypropyl)-*p*-nitrophenyl phosphate were investigated.

Introduction

Bidentate chelate ligand systems with oxygen donor atoms such as β-diketones and their derivatives are widely represented in modern coordination chemistry because they form numerous complexes with s-, p-, d-, and f-metal ions. Lanthanide-based systems $Ln(L)_3$ with these types of ligands demonstrate coordination unsaturation because of the large coordination numbers of lanthanide ions.[1,2] One of the ways to eliminate such unsaturation is the incorporation of additional ligands into the complex molecules. For example, a transition-metal complex with extra donor coordination centers can be used for this purpose. In this regard, much effort has been devoted to the coordination chemistry of tetradentate and hexadentate Salen-like 3d–4f heterobinuclear complexes.[3–6] However, the investigations in the field of 3d–4f heterobinuclear compounds have mainly focused on their applications in magnetism and luminescence,[7–15] whereas their application in areas such as catalysis has, to our knowledge, not been reported.

Recently, we have studied heteroleptic coordination compounds with β-diketone derivatives as carbacylamidophosphates (CAPh), containing the functional fragment C(O)-NHP(O).[16,17] Here, we report the synthesis, structural characterization, and catalytic properties of new binuclear 3d–4f complexes based on unsaturated lanthanide moieties with CAPh, and complexes of Zn^{II} and Ni^{II} with Schiff bases as additional ligands (Scheme 1).

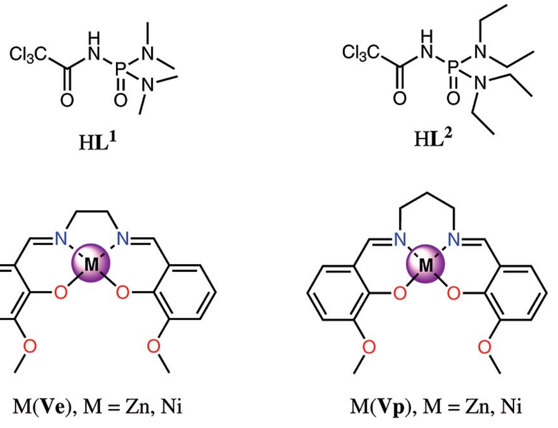

Scheme 1. Precursors for syntheses of 3d–4f complexes.

---

[a] Department of Chemistry, Taras Shevchenko National University of Kyiv,
64/13, Volodymyrska Street, Kyiv 01601, Ukraine
E-mail: alexey.amirkhanov@gmail.com
v_amirkhanov@yahoo.com
www.chem.univ.kiev.ua
[b] Fachbereich Chemie, Universität Konstanz,
78457 Konstanz, Germany
[c] Department of Chemistry of Drugs, Wrocław Medical University,
ul. Borowska 211, 50-552 Wrocław, Poland
[d] SSI "Institute for Single Crystals", National Academy of Science of Ukraine,
60 Lenina Ave., Kharkiv 61001, Ukraine
[e] Department of Inorganic Chemistry, V. N. Karazin Kharkiv National University,
4 Svobody Sq., Kharkiv 61077, Ukraine

Supporting information for this article is available on the WWW under http://dx.doi.org/10.1002/ejic.201402224.

Combining 3d and 4f metals in one molecule, we have tested the ability of the system to catalyze the intramolecular transesterification of 2-(hydroxypropyl)-*p*-nitrophenyl phosphate (HPNP), which has been extensively employed as an RNA model substrate. In many cases, dinuclear species are more reactive than mononuclear species, because one metal ion of the dinuclear system can bind the substrate and the second can bind an OH^- group, which can act as a nucleophile. Various phosphoesterases are known to contain one or more 3d-metal ions within their active site.[18–22] Lanthanide complexes are highly reactive for the cleavage of aryl phosphodiesters[23–25] and diribonucleotides[26] in neutral solutions. With the aim of testing the influence of 3d and 4f metal ions combined in a single molecule, we decided to study our binuclear 3d–4f complexes as catalysts for the hydrolysis of HPNP.

Results and Discussion

Synthesis and Spectroscopic Characterization

With the aim of obtaining new 3d–4f coordination compounds, M(**Ve**) or M(**Vp**) complexes (M = Zn^{II}, Ni^{II}, $H_2\mathbf{Ve}$ = 6,6′-{(1*E*,1′*E*)-[ethane-1,2-diylbis(azanylylidene)]bis(methanylylidene)}bis(2-methoxyphenol) and $H_2\mathbf{Vp}$ = 6,6′-{(1*E*,1′*E*)-[propane-1,3-diylbis(azanylylidene)]bis(methanylylidene)}bis(2-methoxyphenol)) were used as additional ligands for the coordinatively unsaturated $Ln(\mathbf{L}^1)_3$ or $Ln(\mathbf{L}^2)_3$ {$\mathbf{HL}^1$ = *N*-[bis(dimethylamino)phosphoryl]-2,2,2-trichloroacetamide and $\mathbf{HL}^2$ = *N*-[bis(diethylamino)phosphoryl]-2,2,2-trichloroacetamide} unit. The complexes M(**Ve**) and M(**Vp**) were synthesized by the reaction between equimolar amounts of the acetate of 3d-metal and $H_2\mathbf{Ve}$ or $H_2\mathbf{Vp}$ in $CH_3OH/CHCl_3$ and were used for the preparation of 3d–4f complexes without isolation from the reaction mixture. The solution of M(**Ve**) or M(**Vp**) was mixed with a methanol or 2-propanol solution of $Ln(\mathbf{L}^1)_3$ or $Ln(\mathbf{L}^2)_3$, forming Zn–Ln and Ni–Ln complexes containing $Ln(\mathbf{L}^1)_2{}^+$, $Ln(\mathbf{L}^2)_2{}^+$, and $Ln(\mathbf{L}^1)^{2+}$ units. This fact can be explained by the presence of the relatively bulky substituents $N(Me)_2$ and $N(Et)_2$ in $\mathbf{HL}^1$ and $\mathbf{HL}^2$, respectively. The variation of the molar ratio 1:1:3, 1:1:2 and 1:1:1 of the starting compounds $[M(Schiff)/Ln(NO_3)_3/NaL]$ leads to similar results. The synthesized binuclear complexes are summarized in Table 1.

Table 1. Synthesized 3d–4f complexes.

Complexes based on $\mathbf{HL}^1$	
$[Zn(\mu\text{-}\mathbf{Ve})La(\mathbf{L}^1)_2(\mu\text{-}OAc)]$	(**1a**-La)
$[Zn(\mu\text{-}\mathbf{Ve})Eu(\mathbf{L}^1)_2(\mu\text{-}OAc)]MeOH\cdot[Zn(\mu\text{-}\mathbf{Ve})Eu(\mathbf{L}^1)_2(MeOH)(\mu\text{-}OAc)]$	(**1b**-Eu)
$[Ni(\mathbf{Ve})Ln(\mathbf{L}^1)(NO_3)_2]$, Ln = La, Nd	(**1c**-Ln)
Complexes based on $\mathbf{HL}^2$	
$[Zn(\mu\text{-}\mathbf{Ve})Ln(\mathbf{L}^2)_2(\mu\text{-}OAc)]$, Ln = La, Nd, Gd, Er	(**2a**-Ln)
$[Zn(\mu\text{-}\mathbf{Vp})Ln(\mathbf{L}^2)_2(\mu\text{-}OAc)]$, Ln = La, Nd, Eu, Dy, Er, Lu	(**2b**-Ln)
$[Ni(\mu\text{-}\mathbf{Vp})(MeOH)Ln(\mathbf{L}^2)_2(\mu\text{-}OAc)]$, Ln = La, Eu, Gd, Er, Lu	(**2c**-Ln)

Numerous coordination compounds of s-, p-, d- and f-metals based on CAPh have been obtained to date, and it was demonstrated that IR spectroscopy is suitable for a preliminary analysis of the coordination modes of the ligands in these complexes.[27–29]

CAPh ligands in the anionic form coordinate to the metal ions mostly in a bidentate manner through oxygen atoms of the phosphoryl and carbonyl groups with the formation of six-membered chelate cycles, which can be inferred from the bathochromic shifts of the bands of the valence vibrations of phosphoryl ν(PO) and carbonyl ν(CO) groups. In the neutral form, ligands usually coordinate in a monodentate manner. Thus, only the absorption band of the phosphoryl group undergoes the low frequency shift. Interpretation of the IR spectra of the synthesized binuclear compounds based on $\mathbf{HL}^1$ and $\mathbf{HL}^2$ is more complex due to the superposition of the characteristic absorption bands of CAPh ligands and of the Schiff bases. In the IR spectra of the free $\mathbf{HL}^1$ and $\mathbf{HL}^2$, ν(CO) band has a maximum at 1715 cm^{-1} and 1725 cm^{-1}, respectively.[30,31] For the synthesized complexes, an intense asymmetric broad band is observed in the region of 1605–1655 cm^{-1}, which can be related to the superposition of the valence vibrations of ν(CO) [from $(\mathbf{L}^1)^-$ or $(\mathbf{L}^2)^-$] and ν(CN) (from the Schiff bases) (Table S1). In the IR spectra of the neat ligands $\mathbf{HL}^1$ and $\mathbf{HL}^2$, the band of ν(PO) locates at 1205 and 1235 cm^{-1}, respectively. In binuclear complexes, the value of ν(PO) reveals a bathochromic shift and splitting, and falls in the range of 1170–1196 cm^{-1}. Splitting or broadening of the ν(PO) band presumably appears due to non-equivalently coordinated CAPh ligands. The exact assignment of these bands is difficult to achieve without quantum chemical calculations, which is outside the scope of this study. According to the bathochromic shifts for ν(CO) and ν(PO), we assume that $\mathbf{HL}^1$ and $\mathbf{HL}^2$ coordinate to the lanthanide ions in the bidentate mode.

The intense bands with maxima at 1563–1585 cm^{-1} in the IR spectra of **1a**-La, **1b**-Eu, **2a**-Ln, **2b**-Ln, and **2c**-Ln were assigned to $\nu_{as}(CO)$ of the acetate anion.[32,33] In the case of **1c**-La and **1c**-Nd, intense absorption bands in the range of 1292–1472 cm^{-1} indicate the presence of nitrate groups. For the binuclear complexes, broadened bands at 1204–1245 cm^{-1} are observed and assigned to $\nu(C_{Ph}\text{–}O)$ of Zn(Schiff) or Ni(Schiff).[34,35]

The synthesized 3d–4f compounds with diamagnetic Zn^{II} and La^{III} ions were characterized by ^1H and ^{31}P NMR spectroscopy and compared with the corresponding spectra of $\mathbf{HL}^1$, $\mathbf{HL}^2$, $H_2\mathbf{Ve}$, and $H_2\mathbf{Vp}$ (Table S2). In the ^1H NMR spectrum of $\mathbf{HL}^1$, a doublet at $\delta = 2.77$ ppm has a spin-spin coupling constant of 10.4 Hz. In the case of $\mathbf{HL}^2$, a triplet and multiplet are detected at $\delta = 1.15$ and 3.19 ppm, respectively. In the spectrum of **1a**-La, two doublets are observed shifted upfield in comparison with the spectrum of $\mathbf{HL}^1$. This feature relates to the delocalization of π-electron density in the ligand due to deprotonation and coordination to the La^{III} ion. Two doublets in this region might correspond to the presence of nonequivalent phosphoryl ligands in the molecule of the complex. A similar shift of the aliphatic protons is observed in the spectra of complexes **2a**-La and **2b**-La based on HL^2.

Two broad signals in the ^{31}P NMR spectra of **1a**-La, **2a**-La, and **2b**-La additionally confirm the nonequivalence of phosphorus atoms of the coordinated ligands.

In the ^1H NMR spectra of H_2**Ve** and H_2**Vp**, there are four and five types of signals, respectively, assigned to the protons of CH_2, CH_3, CH, and OH groups. Resonance multiplets of the aromatic protons of H_2**Ve** and H_2**Vp** lie in the range of 6.76–6.91 ppm and 6.80–6.94 ppm, respectively. The spectra of **1a**-La, **2a**-La, and **2b**-La contain all expected bands of the Schiff bases. A singlet at 1.8–1.9 ppm clearly indicates the presence of the acetate anion in the complexes. Analysis of the integral intensities of the signals in the ^1H NMR spectra of **1a**-La, **2a**-La, and **2b**-La reveals the formation of the complexes with a molar ratio of the Schiff base to $(\mathbf{L^1})^-$ or $(\mathbf{L^2})^-$ as 1:2.

Crystal Structures of Complexes

Single crystals were obtained for **1a**-La, **1b**-Eu, **1c**-La, **2a**-La, **2b**-La, **2b**-Eu, and **2c**-La complexes. The selected crystallographic data are summarized in Table 2 and Table 3. The molecular structures of the complexes are shown in Figure 1, Figure 2, Figure 3, Figure 4, and Figure 5, Figure S1, and Figure S2, and selected geometrical parameters are listed in Table 4 and Table 5.

Crystal Structures of 1a-La, 2a-La, 2b-La, and 2b-Eu

The crystal structures of the complexes are composed of heterobinuclear units containing Zn^{II} and Ln^{III} ions, which are connected by two bridging phenolate oxygen atoms of $(\mathbf{Ve})^{2-}$ or $(\mathbf{Vp})^{2-}$ and an acetate anion. The $ZnO_2La(Eu)$ fragment is not planar [angle between the O–Zn–O and O–La(Eu)–O planes is 152.3°, 152.8°, 153.3 and 153.9° for **1a**-La, **2a**-La, **2b**-La, and **2b**-Eu, respectively]. The coordination polyhedron of Ln^{III} is formed by four oxygen atoms of Zn(**Ve**) or Zn(**Vp**), four oxygen atoms of bidentately coordinated ligands $(\mathbf{L^1})^-$ or $(\mathbf{L^2})^-$ and an oxygen atom of a bridging linked acetate group, resulting a coordination number of the Ln^{III} ion of nine (Figure 1, Figure 2, Figure S1 and Figure S2).

The average length values of the La–O and Eu–O bonds formed by the bridging phenolate groups are shorter than the bonds observed for the methoxy groups of $(\mathbf{Ve})^{2-}$ or $(\mathbf{Vp})^{2-}$. Similar results were reported for related heterobinuclear β-diketonate complexes.[36] The Zn^{II} ion adopts a tetragonal-pyramidal coordination geometry, where the equa-

Table 2. Crystal data and structure refinement of **1a**-La, **1b**-Eu, **1c**-La.

Compounds	**1a**-La	**1b**-Eu	**1c**-La
Empirical formula	$C_{32}H_{45}Cl_6LaN_8O_{10}P_2Zn$	$C_{66}H_{98}Cl_{12}Eu_2N_{16}O_{22}P_4Zn_2$	$C_{24}H_{30}Cl_3LaN_7NiO_{12}P$
Formula weight	1180.68	2451.54	943.49
Temperature [K]	294(2)	293(2)	293(2)
Wavelength [Å]	0.71073	0.71073	0.71073
Crystal system	monoclinic	triclinic	triclinic
Space group	$P2_1$	$P\bar{1}$	$P\bar{1}$
Unit cell dimensions			
a [Å]	11.656(2)	14.785(3)	9.130(2)
b [Å]	16.249(2)	19.423(2)	11.597(3)
c [Å]	13.366(3)	19.715(2)	18.346(4)
α [°]	90	108.55(4)	91.12(2)
β [°]	108.15(4)	107.02(2)	98.70(2)
γ [°]	90	104.70(3)	110.69(3)
Volume [$Å^3$]	2405.5(7)	4741.7(12)	1790.7(7)
Z	2	2	2
$D_{calcd.}$ [g/cm^3]	1.630	1.717	1.750
Absorption coefficient [mm^{-1}]	1.831	2.284	2.037
$F(000)$	1184	2464	940
Crystal size [mm]	0.40 × 0.20 × 0.10	0.30 × 0.20 × 0.20	0.40 × 0.20 × 0.10
θ range for data collection [°]	2.98–30.00	3.1–27.5	3.01–27.50
Index ranges	$-16 \le h \le 15$, $-22 \le k \le 22$, $-12 \le 1 \le 18$	$-18 \le h \le 19$, $-24 \le k \le 25$, $-25 \le l \le 25$	$-11 \le h \le 11$, $-15 \le k \le 12$, $-23 \le l \le 23$
Reflections collected	25262	41275	14467
Independent reflections	7217	21054	8086
Reflections with $I > 2\sigma(I)$	4853	11014	2632
R(int)	0.0320	0.0627	0.1155
Restraints/parameters	14/565	7/1105	5/448
Goodness-of-fit on F^2	0.880	0.787	0.608
Final R indices [$I > 2\sigma(I)$]	R_1 = 0.0470, wR_2 = 0.1029	R_1 = 0.0489, wR_2 = 0.0804	R_1 = 0.0552, wR_2 = 0.0630
R indices (all data)	R_1 = 0.0735, wR_2 = 0.1111	R_1 = 0.0726, wR_2 = 0.1098	R_1 = 0.1858, wR_2 = 0.0798
Largest diff. peak and hole [e Å^{-3}]	1.08 and –0.43	1.435 and –1.248	0.920 and –0.674
CCDC reference number	985567	985568	985564

Table 3. Crystal data and structure refinement of **2a**-La, **2b**-La, **2b**-Eu, and **2c**-La.

Compounds	**2a**-La	**2b**-La	**2b**-Eu	**2c**-La
Empirical formula	$C_{40}H_{61}Cl_6LaN_8O_{10}P_2Zn$	$C_{41}H_{63}Cl_6LaN_8O_{10}P_2Zn$	$C_{41}H_{63}Cl_6EuN_8O_{10}P_2Zn$	$C_{42}H_{67}Cl_6LaN_8O_{11}P_2Ni$
Formula weight	1292.89	1306.91	1319.96	1332.30
Temperature [K]	293(2)	100(2)	293(2)	294(2)
Wavelength [Å]	0.71073	0.71073	0.71073	0.71073
Crystal system	orthorhombic	monoclinic	monoclinic	monoclinic
Space group	$P2_12_12_1$	$P2_1/c$	$P2_1/c$	$P2_1/n$
Unit cell dimensions				
a [Å]	14.794(2)	15.5670(5)	15.860(2)	13.849(3)
b [Å]	16.368(3)	22.8383(9)	22.508(2)	29.583(2)
c [Å]	23.092(3)	15.4462(5)	15.231(3)	15.064(2)
α [°]	90	90	90	90
β [°]	90	93.839(3)	92.01(3)	108.18(3)
γ [°]	90	90	90	90
Volume [Å^3]	5591.7(15)	5479.2(3)	5433.8(14)	5863.6(15)
Z	4	4	4	4
$D_{\text{calcd.}}$ [g/cm^3]	1.536	1.584	1.614	1.509
Absorption coefficient [mm^{-1}]	1.583	1.616	1.998	1.426
F(000)	2624	2656	2680	2720
Crystal size [mm]	0.40 × 0.20 × 0.10	0.20 × 0.05 × 0.05	0.40 × 0.20 × 0.10	0.40 × 0.20 × 0.10
θ range for data collection [°]	2.92–30.00	2.87–27.50	2.93–27.50	2.93–30.00
Index ranges	$-20 \le h \le 18$, $-22 \le k \le 23$, $-32 \le l \le 32$	$-20 \le h \le 20$, $-27 \le k \le 29$, $-11 \le l \le 20$	$-20 \le h \le 20$, $-29 \le k \le 29$, $-19 \le l \le 19$	$-19 \le h \le 19$, $-41 \le k \le 21$, $-19 \le l \le 21$
Reflections collected	56429	35115	44805	58654
Independent reflections	8815	12469	11765	16929
Reflections with $I > 2\sigma(I)$	6291	8260	4888	11249
R(int)	0.1446	0.0801	0.1745	0.0424
Restraints/parameters	35/691	0/633	16/620	18/698
Goodness-of-fit on F^2	0.936	1.038	0.880	0.922
Final R indices [$I > 2\sigma(I)$]	$R_1 = 0.0506$, $wR_2 = 0.1092$	$R_1 = 0.0640$, $wR_2 = 0.1235$	$R_1 = 0.097$, $wR_2 = 0.1942$	$R_1 = 0.0384$, $wR_2 = 0.0729$
R indices (all data)	$R_1 = 0.0720$, $wR_2 = 0.1150$	$R_1 = 0.1116$, $wR_2 = 0.1374$	$R_1 = 0.1931$, $wR_2 = 0.2166$	$R_1 = 0.0722$, $wR_2 = 0.0787$
Largest diff. peak and hole [e Å^{-3}]	1.165 and –1.487	1.968 and –1.022	5.836 and –1.680	0.821 and –0.614
CCDC reference number	985566	985565	985570	985569

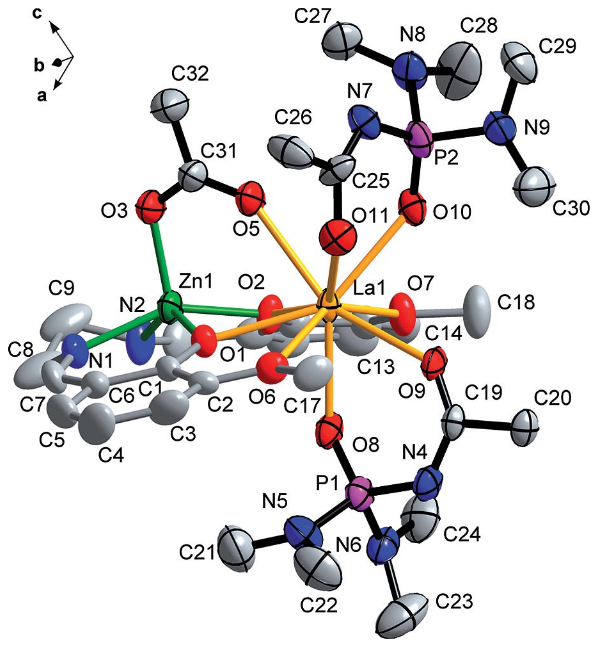

Figure 1. Molecular structure of **1a**-La with atom numbering scheme and 30% probability thermal ellipsoids. Hydrogen and chlorine atoms are omitted for clarity.

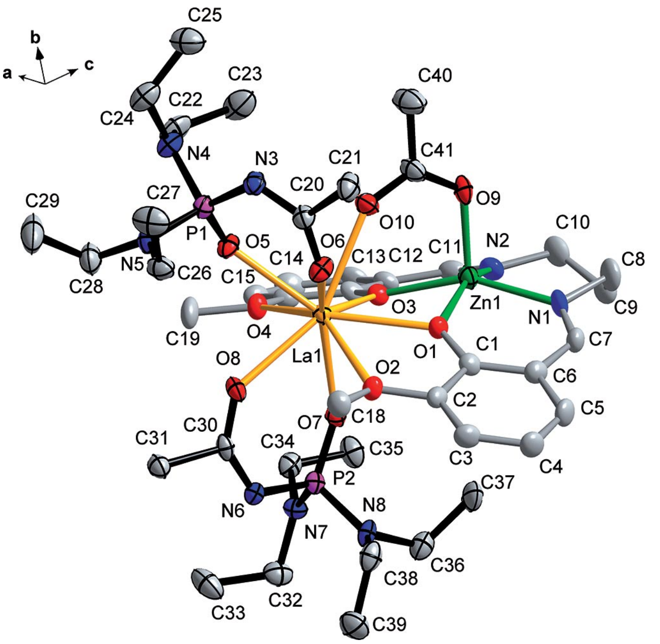

Figure 2. Molecular structure of **2b**-La with atom numbering scheme and 50% probability thermal ellipsoids. Hydrogen and chlorine atoms are omitted for clarity.

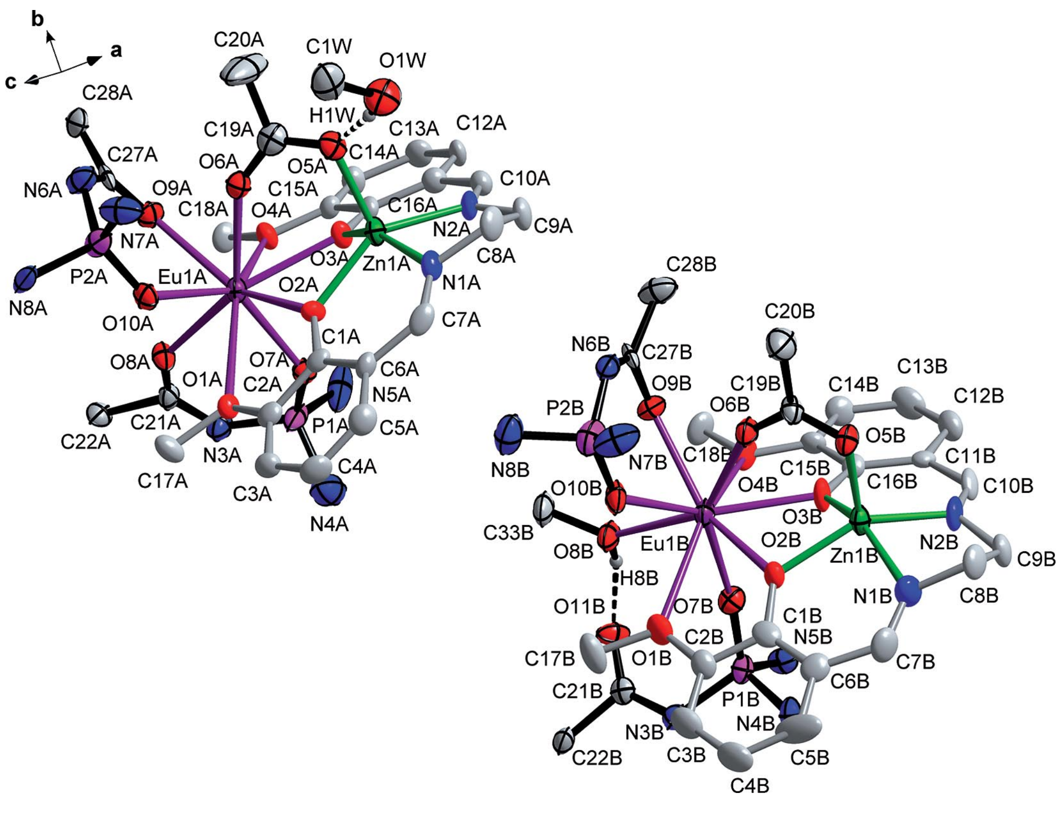

Figure 3. Molecular structure of **1b**-Eu with atom numbering scheme and 50% probability thermal ellipsoids. Hydrogen atoms not involved in hydrogen bonding, chlorine, and carbon atoms of $N(CH_3)_2$ groups are omitted for clarity.

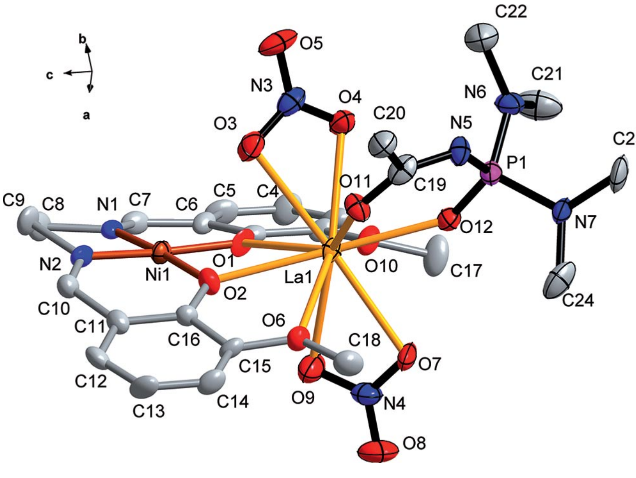

Figure 4. Molecular structure of **1c**-La with atom numbering scheme and 30% probability thermal ellipsoids. Hydrogen and chlorine atoms are omitted for clarity.

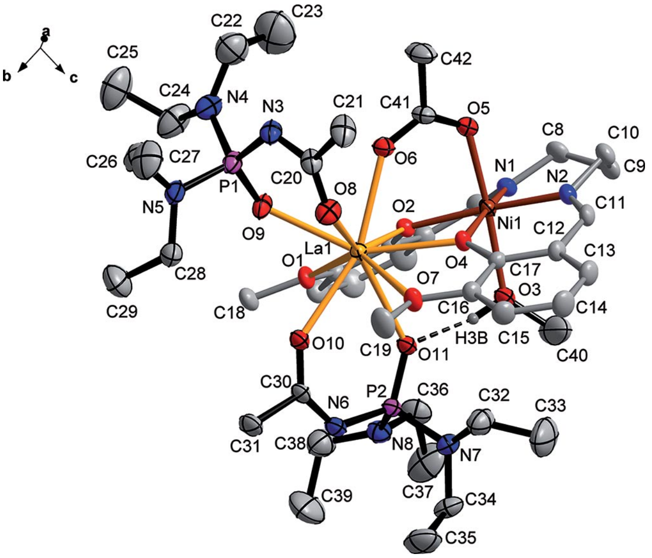

Figure 5. Molecular structure of **2c**-La with atom numbering scheme and 30% probability thermal ellipsoids. Hydrogen atoms not involved in hydrogen bonding and chlorine atoms are omitted for clarity.

torial positions are occupied by two nitrogen and two oxygen atoms of $(\mathbf{Ve})^{2-}$ or $(\mathbf{Vp})^{2-}$, whereas the axial position is occupied by the oxygen atom of the acetate anion. The Zn^{II} ion is displaced from the N_2O_2 plane by 0.566, 0.578, 0.466 and 0.453 Å for **1a**-La, **2a**-La, **2b**-La, and **2b**-Eu, respectively. The bond lengths in the fragments Zn(**Ve**) and Zn(**Vp**) are comparable to the published data for similar complexes.[37–39]

In the complexes, **1a**-La, **2a**-La, and **2b**-Eu, some of the carbon and chlorine atoms are disordered over two positions: C8–C9 (0.25:0.75) for **1a**-La, Cl4–Cl6 (0.4:0.6), C8–C9 (0.4:0.6), C31–C32 (0.3:0.7), C33 (0.4:0.6), C34 (0.25:0.75), C35–C36 (0.5:0.5) for **2a**-La, and C22–C23 (0.3:0.7), C24 (0.35:0.65), C25(0.5:0.5), C36 (0.15:0.85), C37 (0.35:0.65) for **2b**-Eu.

Table 4. Selected bond lengths of **1a**-La, **1b**-Eu, and **1c**-La.

1a-La		**1b**-Eu				**1c**-La	
		A		B			
La1–Zn1	3.465(2)	Eu1A–Zn1A	3.3960(9)	Eu1B–Zn1B	3.393(1)	La1–Ni1	3.575(1)
La1–O6	2.792(5)	Eu1A–O1A	2.723(4)	Eu1B–O1B	2.729(4)	La1–O6	2.715(4)
La1–O1	2.495(6)	Eu1A–O2A	2.388(3)	Eu1B–O2B	2.387(4)	La1–O2	2.560(4)
La1–O2	2.496(6)	Eu1A–O3A	2.378(3)	Eu1B–O3B	2.391(3)	La1–O1	2.581(4)
La1–O7	2.727(6)	Eu1A–O4A	2.657(4)	Eu1B–O4B	2.675(4)	La1–O10	2.721(5)
La1–O8	2.457(5)	Eu1A–O7A	2.372(4)	Eu1B–O7B	2.320(4)	La1–O12	2.431(4)
La1–O10	2.489(6)	Eu1A–O10A	2.346(3)	Eu1B–O10B	2.376(3)	La1–O11	2.459(5)
La1–O9	2.531(4)	Eu1A–O8A	2.372(3)	Eu1B–O8B	2.421(3)	La1–O3	2.685(5)
La1–O11	2.488(7)	Eu1A–O9A	2.413(4)	Eu1B–O9B	2.377(4)	La1–O4	2.607(5)
La1–O5	2.559(5)	Eu1A–O6A	2.436(4)	Eu1B–O6B	2.417(4)	La1–O7	2.618(5)
Zn1–O1	2.011(6)	Zn1A–O2A	2.021(3)	Zn1B–O2B	2.026(3)	La1–O9	2.653(6)
Zn1–O2	1.999(6)	Zn1A–O3A	2.004(3)	Zn1B–O3B	2.001(4)	Ni1–O1	1.836(5)
Zn1–N1	2.019(8)	Zn1A–N1A	2.025(5)	Zn1B–N1B	2.036(6)	Ni1–O2	1.810(5)
Zn1–N2	2.063(8)	Zn1A–N2A	2.055(4)	Zn1B–N2B	2.042(4)	Ni1–N1	1.858(6)
Zn1–O3	1.980(5)	Zn1A–O5A	1.988(4)	Zn1B–O5B	1.999(4)	Ni1–N2	1.814(6)

Table 5. Selected bond lengths of **2a**-La, **2b**-La, **2b**-Eu, and **2c**-La.

2a-La		**2b**-La		**2b**-Eu		**2c**-La	
La1–Zn1	3.480(1)	La1–Zn1	3.595(1)	Eu1–Zn1	3.508(2)	La1–Ni1	3.526(1)
La1–O1	2.737(4)	La1–O2	2.678(3)	Eu1–O1	2.619(7)	La1–O1	2.687(2)
La1–O2	2.496(4)	La1–O1	2.498(3)	Eu1–O2	2.391(8)	La1–O2	2.470(2)
La1–O3	2.501(4)	La1–O3	2.532(4)	Eu1–O3	2.429(8)	La1–O4	2.454(2)
La1–O4	2.730(4)	La1–O4	2.651(3)	Eu1–O4	2.605(7)	La1–O7	2.697(2)
La1–O8	2.434(4)	La1–O5	2.478(3)	Eu1–O5	2.357(8)	La1–O9	2.481(2)
La1–O11	2.456(3)	La1–O7	2.458(4)	Eu1–O7	2.366(7)	La1–O11	2.626(2)
La1–O9	2.520(4)	La1–O6	2.517(4)	Eu1–O6	2.446(7)	La1–O8	2.511(2)
La1–O10	2.503(3)	La1–O8	2.535(4)	Eu1–O8	2.408(8)	La1–O10	2.541(2)
La1–O7	2.551(4)	La1–O10	2.530(4)	Eu1–O9	2.455(8)	La1–O6	2.497(2)
Zn1–O2	1.996(5)	Zn1–O1	2.073(4)	Zn1–O2	2.057(9)	Ni1–O2	2.052(2)
Zn1–O3	2.005(4)	Zn1–O3	2.050(3)	Zn1–O3	2.067(8)	Ni1–O4	2.034(2)
Zn1–N1	2.064(8)	Zn1–N1	2.085(4)	Zn1–N1	2.08(1)	Ni1–N1	2.051(2)
Zn1–N2	2.051(7)	Zn1–N2	2.119(5)	Zn1–N2	2.063(9)	Ni1–N2	2.034(2)
Zn1–O5	1.970(4)	Zn1–O9	1.964(4)	Zn1–O10	1.952(9)	Ni1–O5	2.028(2)
						Ni1–O3	2.167(2)

Crystal Structure of 1b-Eu

Despite the identical method of synthesis of **1a**-La and **1b**-Eu, the molecular structures of the complexes differ. In the latter, the asymmetric unit contains two independent molecules **A** and **B** with different coordination environments of the $\mathrm{Eu^{III}}$ ion (Figure 3).

The coordination environment of the $\mathrm{Eu^{III}}$ ion in molecule **A** of **1b**-Eu is similar to that of **1a**-La. The acetate group in **A** additionally forms an intermolecular O–H···O′ hydrogen bond with the hydrogen atom of a non-coordinated molecule of methanol (H···O′ 1.99 Å, O–H···O′ 172°). In the case of **B**, the coordination sphere of $\mathrm{EuO_9}$ is formed by four oxygen atoms of Zn(**Ve**), three oxygen atoms of bidentately and monodentately coordinated $(\mathbf{L^1})^-$ ligands, and one oxygen atom of coordinated methanol. An oxygen atom of the bridged acetate anion occupies the ninth position. Furthermore, an intramolecular hydrogen bond between the CO group of the monodentate coordinated $(\mathbf{L^1})^-$ and the coordinated methanol molecule is observed (H···O′ 1.84 Å, O–H···O′ 161°) in molecule **B**. The coordination polyhedra of $\mathrm{La^{III}}$ (**1a**-La) and $\mathrm{Eu^{III}}$ (**1b**-Eu) ions represent a distorted tricapped trigonal prism and a distorted monocapped square antiprism, respectively, according to the geometrical standards of Guggenberger.[40] The coordination number of the $\mathrm{Zn^{II}}$ ion is five, and the coordination environment is a slightly distorted tetragonal-pyramidal ($\mathrm{O_3N_2}$) for both molecules. The equatorial plane of the pyramid is formed by two oxygen and two nitrogen atoms of $(\mathbf{Ve})^{2-}$, the axial position is occupied by the oxygen atom of the acetate group. The deviation of $\mathrm{Zn^{II}}$ ion from the mean $\mathrm{N_2O_2}$ plane is 0.568 and 0.582 Å for **A** and **B** molecules, respectively. The angles between the (OZnO) and (OEuO) planes containing the bridging oxygen atoms are 150.9° and 150.5° for **A** and **B** molecules, respectively. In the complex, **1b**-Eu, some of the carbon atoms are disordered over two positions: C8B–C9B (0.5:0.5).

Crystal Structure of 1c-La

The crystal structure of the complex consists of heterobinuclear molecules $[\mathrm{Ni}(\mathbf{Ve})\mathrm{La}(\mathbf{L^1})(\mathrm{NO_3})_2]$ in which the $\mathrm{La^{III}}$ center has a decacoordination environment. In addition to the phenolate and methoxy oxygen atoms of Ni(**Ve**), four oxygen atoms of two bidentately coordinated nitrate groups and two O atoms of bidentately coordinated $(\mathbf{L^1})^-$ complete the coordination sphere (Figure 4). The La–O bond lengths of the four types are significantly different: the longest are the La–O(methoxy) distances and the shortest are the La–O(P) (see Table 4). The $\mathrm{Ni^{II}\cdots La^{III}}$ separation is 3.575(1) Å. The $\mathrm{Ni^{II}}$ ion is tetracoordinate by two imine nitrogen atoms and two bridging phenolate oxygen atoms from the $(\mathbf{Ve})^{2-}$ anion and adopts a slightly distorted square-planar geometry. The $\mathrm{Ni^{II}}$ center deviates from the N_2O_2 plane by 0.005 Å. As expected, the Ni–N and Ni–O bond lengths are quite similar to those of the individual complex [Ni(**Ve**)-H_2O].[41] The angle between the (ONiO) and (OLaO) planes involving two bridging oxygen atoms is 164.3°, and is larger than in **1a**-La, **1b**-Eu, **2a**-La, **2b**-La, and **2b**-Eu compounds.

Crystal Structure of 2c-La

The structural determination of **2c**-La shows the existence of a heterodinuclear complex [Ni(μ-**Vp**)(MeOH)-La$(\mathbf{L^2})_2$(μ-OAc)] (Figure 5). The $\mathrm{La^{III}}$ ion is nine-coordinate by four oxygen atoms from the bridging Schiff base, four oxygen atoms from two bidentate chelating $(\mathbf{L^2})^-$ ligands and the oxygen atom of the bridging acetate anion, forming a distorted monocapped square-antiprismatic coordination environment. The position of the facet is occupied by the oxygen atom O7 of the $(\mathbf{Vp})^{2-}$ ligand. An intramolecular O–H···O hydrogen bond is observed between the PO group and the coordinated methanol molecule. The Ni···La separation is 3.526(1) Å.

Two La–O(P) bond lengths of the $(\mathbf{L^2})^-$ are not equal [2.481(2) and 2.626(2) Å] and this difference might be explained by the participation of one of the PO group in the formation of the hydrogen bond.

The $\mathrm{Ni^{II}}$ ion is coordinated by two oxygen atoms and two nitrogen atoms of the Schiff base. The methanol molecule and the bridging acetate ligand complete formation of a slightly distorted octahedral sphere N_2O_4. The $\mathrm{Ni^{II}}$ center is displaced from the equatorial mean plane of N_2O_2 by 0.081 Å. The value of the angle between the Ni1–O2–O4 and La1–O2–O4 planes is 167.5°, which is larger than those of $\mathrm{Zn^{II}}$-containing complexes **2b**-La and **2b**-Eu, thus the $\mathrm{NiO_2La}$ fragment is less bent.

From the literature data, it is known that the $\mathrm{Ni^{II}}$ ion has an octahedral environment in the case of $(\mathbf{Vp})^{2-}$ complexes[42–44] and a square-planar or pyramidal geometry when $(\mathbf{Ve})^{2-}$ is used as precursor,[45] which correlates well with our data.

In the complex **2c**-La, atoms Cl4–Cl6 and C36–C37 are disordered over two positions with equal occupancy ratios (0.5:0.5).

Mass-Spectrometric Analysis of 2b-Nd, 2c-La, and 2c-Er

To study in solution the stability of the obtained binuclear coordination compounds based on $\mathbf{HL^2}$ ligand, ESI MS studies of **2b**-Nd, **2c**-La, and **2c**-Er were undertaken in acetonitrile.

The ESI mass spectrum of the complex **2b**-Nd in the positive range contains a signal with *m*/*z* 1252, assigned to the moiety $[\mathrm{Zn}(\mathbf{Vp})\mathrm{Nd}(\mathbf{L^2})_2{}^+]^+$ (M_{calc} = 1252.05). The experimentally observed isotope distribution in this spectrum is in good agreement with the calculated model for the corresponding species (Figure S3).

Mass spectra of the coordination compounds **2c**-La and **2c**-Er indicate peaks with *m*/*z* 1241 and 1268, respectively, which were also assigned to the species $[\mathrm{Ni}(\mathbf{Vp})\mathrm{La}(\mathbf{L^2})_2{}^+]^+$ (M_{calc} = 1241.05) and $[\mathrm{Ni}(\mathbf{Vp})\mathrm{Er}(\mathbf{L^2})_2{}^+]^+$ (M_{calc} = 1268.08) (Figure S4, Figure S5).

Thus, the ESI mass spectrometric studies in acetonitrile of the synthesized complexes confirm the existence in solution of heterodinuclear fragments comprising $(\mathbf{Vp})^{2-}$ ligand and phosphoryl ligands.

Kinetic Measurements

Intramolecular transesterification of the phosphodiester 2-(hydroxypropyl)-*p*-nitrophenyl phosphate (HPNP) provides an excellent test for catalysis because the substrate is easily available and 4-nitrophenolate product (NP) can be detected spectrophotometrically (Scheme 2). $\mathrm{Ln^{III}}$ and 3d-metal mediated hydrolytic reactions, including phosphatase-like activity, were studied in buffered aqueous solutions (or in media with high water content) to closely mimic biological conditions.[46–48]

An initial screening of the hydrolytic activity of **2b**-Ln and **2c**-Ln was carried out at pH 8.00, in dimethyl sulfoxide (DMSO)/buffered water (1:1, v/v) at 25 °C, where $\mathrm{Ln^{III}}$ is $\mathrm{La^{III}}$, $\mathrm{Eu^{III}}$, or $\mathrm{Lu^{III}}$. These conditions roughly corresponded to the maximum hydrolysis rates of the substrate, as follows from bell-shaped pH profiles: Figure 6 shows the pH profile for **2b**-Eu. The DMSO/buffered water (1:1, v/v) system was chosen because the compounds had low solubility in water.

The rate constants for the HPNP hydrolysis were obtained by plotting the increase of NP absorbance at 405 nm as a function of time. The kinetic data for all complexes show that the rate of hydrolysis is linearly dependent on the complex concentration (Figure 7). Pseudo-first-order rate constants k_{obs} defined by $V_0 = k_{obs}[\text{complex}]_0$. The results (Table 6) show that **2b**-Lu is the most effective among the

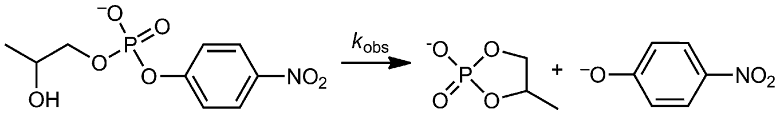

Scheme 2. Intramolecular hydrolytic degradation of the 2-(hydroxypropyl)-*p*-nitrophenyl phosphate (HPNP) resulting in formation of the cyclic phosphate (3-methyl-2,5-dioxaphospholan-2-ol 2-oxide) and the *p*-nitrophenolate ion.

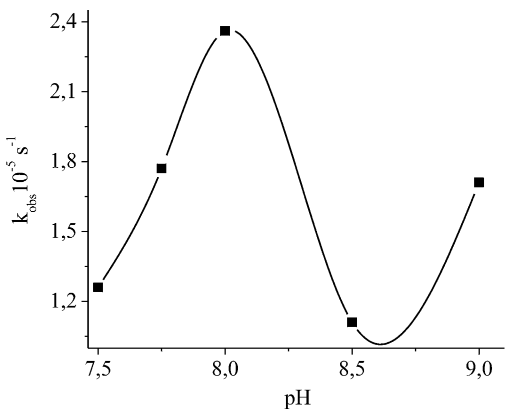

Figure 6. Effect of pH on HPNP hydrolysis rate mediated by **2b**-Eu. $[HPNP]_0$ = 0.16 mм, $[$**2b**-Eu$]_0$ = 0–0.16 mм at 25 °C, in DMSO/buffered H_2O (1:1).

examined complexes. Calculated k_{obs} for **2b**-Ln and **2c**-Ln lay in the order Lu > Eu > La and were comparable to those found for the phosphodiester and DNA hydrolysis promoted by di- and multi-nuclear metal complexes.[47,49–51] No significant hydrolysis of the test substrate occurred in the absence of the complexes.

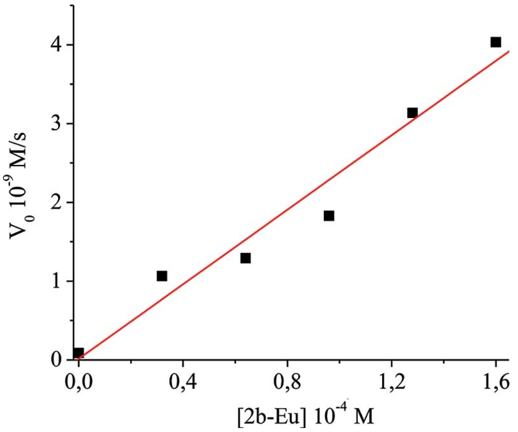

Figure 7. Dependence of the reaction rate on the concentration of the complex **2b**-Eu for the hydrolysis of HPNP; $[HPNP]_0$ = 0.16 mм, at 25 °C, pH 8.00, in DMSO/Tris·HCl buffer (1:1).

To further study the effect of the HPNP concentration on phosphodiester hydrolysis catalyzed by **2b**-Ln and **2c**-Ln, kinetic data analyses were performed by using the Michaelis–Menten method. As an example, the plot of the initial reaction rate vs. the concentration of the substrate for **2b**-Eu is shown in Figure 8.

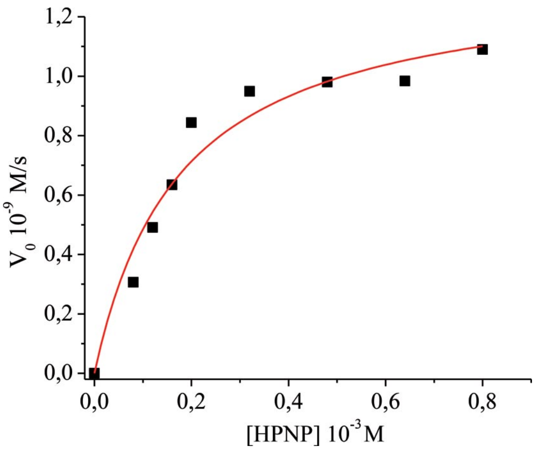

Figure 8. Dependence of the initial reaction rate (V_0) on the HPNP concentration for the hydrolysis reaction promoted by **2b**-Eu on concentration; $[$**2b**-Eu$]_0$ = 8 × 10^{-6} м, at 25 °C, pH 8.00, in DMSO/Tris·HCl buffer (1:1).

The kinetic data for other compounds are summarized in Table 6. The initial reaction rate vs. concentration of HPNP increases, suggesting formation of a complex–substrate intermediate. Analysis of the data for **2c**-Lu reveals that the Michaelis–Menten constant (K_M = 0.47 ± 0.09 mм) is higher than other studied complexes, indicating less binding affinity and therefore a higher catalytic rate constant [k_{cat} = (2.86 ± 0.20) × 10^{-4} s^{-1}]. The highest binding affinity was observed for **2c**-La (K_M = 0.05 ± 0.01 mм). Complexes **2b**-Lu and **2c**-Lu showed higher catalytic efficiency than the complexes of La^{III} and Eu^{III}. These three lanthanides have the same electron charge, but because it has the smallest radius, Lu^{III} is the stronger Lewis acid, which presumably helps to deprotonate the coordinated water molecule forming an active hydroxyl group. The effect of 3d-metal ion may be associated with a ligand substitution mechanism: the five-coordinate Zn^{II} ion undergoes associative substitution but the six-coordinate Ni^{II} ion follows dissociative substitution. This difference results in higher values for k_{obs} for **2b**-Ln compared with those for **2c**-Ln (Table 6).

The kinetic studies on the catalytic properties of the studied complexes suggest that the combination of different metal ions and types of ligands may enable the design of highly efficient mimics of the hydrolytic enzyme.

Table 6. Kinetic data calculated for reactions of HPNP catalytic hydrolysis.

Complex	k_{obs} [s^{-1}]	k_{obs}/k_{uncat}	k_{cat} [s^{-1}]	K_m [mм]	k_{cat}/K_M [$s^{-1}M^{-1}$]
2b-La	(7.44 ± 0.18) × 10^{-6}	(5.3 ± 0.1) × 10^4	(1.08 ± 0.04) × 10^{-4}	0.11 ± 0.01	0.80 ± 0.11
2b-Eu	(2.35 ± 0.38) × 10^{-5}	(1.7 ± 0.3) × 10^5	(1.68 ± 0.14) × 10^{-4}	0.18 ± 0.04	0.50 ± 0.01
2b-Lu	(3.36 ± 0.12) × 10^{-5}	(2.4 ± 0.1) × 10^5	–	–	0.69 ± 0.15
2c-La	(6.16 ± 0.53) × 10^{-6}	(4.4 ± 0.4) × 10^4	(9.46 ± 0.40) × 10^{-5}	0.05 ± 0.01	0.50 ± 0.10
2c-Eu	(1.07 ± 0.09) × 10^{-5}	(7.6 ± 0.6) × 10^4	(9.39 ± 0.50) × 10^{-5}	0.18 ± 0.03	0.24 ± 0.04
2c-Lu	(1.61 ± 0.10) × 10^{-5}	(1.2 ± 0.1) × 10^5	(2.86 ± 0.20) × 10^{-4}	0.47 ± 0.09	0.85 ± 0.07
no catalyst	1,4 × 10^{-10}	1			

Conclusions

We have reported the synthesis and crystal studies of six new types of 3d–4f heterobinuclear complexes based on carbacylamidophosphates $Cl_3CC(O)NHP(O)[N(Me)_2]_2$ and $Cl_3CC(O)NHP(O)[N(Et)_2]_2$ and Schiff base ligand systems. It was shown that the crystal structures of the complexes are composed of M(**Ve**) or M(**Vp**) (M = Zn^{II}, Ni^{II}) moieties and Ln-containing motifs forming together heterobinuclear molecules. For most of complexes, metal ions are connected by two bridging phenolate oxygen atoms of (**Ve**)$^{2-}$ or (**Vp**)$^{2-}$ and an acetate group. The coordination number of Ln^{III} and Zn^{II} ions is nine and five, respectively. In the case of **1c**-La, the Ni^{II} ion is tetracoordinated by two imine nitrogen atoms and two bridging phenolate oxygen atoms from the (**Ve**)$^{2-}$ anion; the La^{III} center is ten-coordinated. In the complex **2c**-La, the Ni^{II} ion is six-coordinate, whereas the coordination number of La^{III} ion is nine. To the best of our knowledge, the ability of the obtained 3d–4f complexes to promote phosphodiester hydrolysis using the RNA mimic substrate HPNP was demonstrated for the first time. The kinetic data show that the rate of hydrolysis is linearly dependent on complex concentration. Calculated rate constants k_{obs} for **2b**-Ln and **2c**-Ln follow the order Lu > Eu > La, where **2b**-Lu is the most effective, giving five orders of magnitude improvement in the rate of the catalyzed reaction compared with the noncatalyzed reaction. The different ligand substitution mechanism for Ni^{II} or Zn^{II} ions can presumably influence k_{obs} values for the corresponding complexes.

Experimental Section

Materials and Methods: All starting reagents used in this work were obtained from commercial sources and used without further purification. IR measurements were performed with a Perkin–Elmer Spectrum BX spectrometer on samples in the form of KBr pellets. NMR spectra were recorded with a Varian Mercury 400 NMR spectrometer at 25 °C. ^1H and ^{31}P NMR spectra were recorded at 400 and 162.1 MHz, respectively. Chemical shifts are reported with reference to $SiMe_4$ (^1H) and H_3PO_4 (^{31}P). Elemental analyses (C, H, N) were performed with an EL III Universal CHNOS Elemental Analyzer. ESI MS were obtained with a Bruker APEX IV spectrometer. Predicted isotopic splitting patterns of peaks were calculated by using the program Isopro 3.1.

Kinetic Measurements: Kinetic measurements were recorded with a Varian Cary 50 UV/Vis spectrophotometer at 25 °C, in 3 mL reaction volumes using buffered solutions in DMSO/water (1:1); 2-amino-2-hydroxymethylpropane-1,3-diol hydrochloride (Tris·HCl) was used as a buffer. The reported results were obtained by averaging of at least three independent measurements. In a typical experiment, aqueous buffer solution (1.5 mL) was mixed with complex stock solution (in DMSO, 0.5 mL) and DMSO (0.5 mL) in a temperature-controlled spectrophotometric cell. After equilibration for 5 min, HPNP substrate stock solution (in DMSO, 0.5 mL) was added and data collection was started immediately. The cleavage of substrate was monitored by following the increase of the 4-nitrophenolate absorption at 405 nm. The activities of the complexes were determined by the method of initial rates, taking into account the molar absorptivity of the product at the corresponding pH value.[51] Conversion from absorbance to concentration was performed by using the Lambert–Beer law. Kinetic parameters (k_{cat} and K_M) were obtained by fitting the data to the Michaelis–Menten equation: [$V_0 = k_{cat}(\text{complex})_0[S]_0/(K_M + [S]_0)$], and k_{cat}/K_M values were obtained by fitting the linear portion of the plot to $V_0 = (k_{cat}/K_M)[\text{complex}]_0[S]_0$.

X-ray Structure Determination: Crystal data were collected with an Xcalibur-3 diffractometer (graphite monochromated Mo-K_α radiation, CCD detector, ϕ and ω-scanning). The structures were solved by the direct method using the SHELXTL package.[52] Full-matrix least-squares refinement against F^2 in anisotropic approximation for non-hydrogen atoms was used. Positions of the hydrogen atoms were located from electron density difference maps and refined by the “riding” model with $U_{iso} = nU_{eq}$ of the carrier atom (n = 1.5 for methyl groups and n = 1.2 for other hydrogen atoms).

CCDC-985564 (for **1a**-La), -985565 (for **1b**-Eu), -985566 (for **1c**-La), -985567 (for **2a**-La), -985568 (for **2b**-La), -985569 (for **2b**-Eu), and -985570 (for **2c**-La) contain the supplementary crystallographic data for the paper. These data can be obtained free of charge from The Cambridge Crystallographic Data Centre via www.ccdc.cam.ac.uk/data_request/cif.

Syntheses

Synthesis of HL^1, HL^2, NaL^1, and NaL^2: Compounds HL^1 and HL^2 were prepared and identified according to reported procedures.[30,31] The sodium salts NaL^1 and NaL^2 were prepared by reaction between equimolar amounts of sodium methylate and HL^1 or HL^2 in methanol medium and were used for preparation of complexes without isolation from the reaction mixture. In the case of Ni(**Ve**)-containing binuclear complexes, NaL^2 were used in the same way, but obtained in 2-propanol medium starting from sodium isopropylate.

Synthesis of H_2Ve, H_2Vp, M(Ve), and M(Vp) (M = Zn^{II}, Ni^{II})

The Schiff bases H_2**Ve** and H_2**Vp** were synthesized straightforwardly by condensation of 2-hydroxy-3-methoxybenzaldehyde and the appropriate diamine (ethane-1,2-diamine or propane-1,3-diamine).[53,54]

The complexes M(**Ve**) and M(**Vp**) (M = Zn^{II}, Ni^{II}), were obtained by reaction between methanol solution (2 mL) of zinc acetate $Zn(OAc)_2\cdot 2H_2O$ (0.1097 g, 0.5 mmol) or $Ni(OAc)_2\cdot 4H_2O$ (0.1244 g, 0.5 mmol) and a solution of H_2**Ve** (H_2**Vp**) [0.1642 g (0.1712 g), 0.5 mmol] in chloroform (3 mL) and were used for the preparation of binuclear complexes without isolation in the individual state.

1a-La and 1b-Eu: Hydrated nitrate $Ln(NO_3)_3\cdot xH_2O$ (0.5 mmol) was dissolved in methanol (2 mL) and mixed with NaL^1 (1 mmol) in methanol (3 mL). The mixture was added dropwise with constant stirring to a hot solution of Zn(**Ve**) (0.5 mmol) and heated to reflux for 1.5 h. The resulting solution was left in air at room temperature and crystals of **1a**-La and **1b**-Eu, which formed after 7–9 days, were filtered, washed with cold acetone and diethyl ether, and dried in air. Yield: 60–75%. **1a**-La: $C_{32}H_{45}Cl_6LaN_8O_{10}P_2Zn$ (1180.71): calcd. C 32.55, H 3.84, N 9.49; found C 32.47, H 3.87, N 9.52. **1b**-Eu: $C_{66}H_{98}Cl_{12}Eu_2N_{16}O_{22}P_4Zn_2$ (2451.61): calcd. C 32.33, H 4.03, N 9.14; found C 32.62, H 4.09, N 9.18.

1c-Ln, Ln = La, Nd: Hydrated nitrate $Ln(NO_3)_3\cdot xH_2O$ (0.5 mmol) was dissolved in 2-propanol (2 mL) and mixed with NaL^1 (0.5 mmol) in 2-propanol (3 mL). The sodium nitrate was filtered off and the resulting solution was added dropwise with constant stirring to a hot solution of Ni(**Ve**) (0.5 mmol) and heated to reflux for 3 h. The resulting light-orange precipitate was filtered off, dried in air, and dissolved in a mixture of acetonitrile and chloroform

(5:1) upon heating. The solution was left to evaporate slowly in air at room temperature and crystals of **1c**-La and a crystalline powder of **1c**-Nd, which were formed after 7–10 days, were filtered, washed with cold acetone and diethyl ether, and dried in air. Yield: 50–60%. **1c**-La: $C_{24}H_{30}Cl_3LaN_7NiO_{12}P$ (943.49): calcd. C 30.55, H 3.21, N 10.39; found C 30.47, H 3.25, N 10.41. **1c**-Nd: $C_{24}H_{30}Cl_3N_7NdNiO_{12}P$ (948.82): calcd. C 30.38, H 3.19, N 10.33; found C 30.43, H 3.29, N 10.23.

2a-Ln, Ln = La, Nd, Gd, Er: Prepared by following the procedure described for **1a**-Ln using **HL**^{2} as the staring ligand. Crystals of **2a**-La and powders of **2a**-Nd, **2a**-Gd, and **2a**-Er formed after 5–7 days. Yield: 70–85%. **2a**-La: $C_{40}H_{61}Cl_6LaN_8O_{10}P_2Zn$ (1292.92): calcd. C 37.16, H 4.76, N 8.67; found C 37.28, H 4.69, N 8.71. **2a**-Nd: $C_{40}H_{61}Cl_6N_8NdO_{10}P_2Zn$ (1298.26): calcd. C 37.01, H 4.74, N 8.63; found C 37.06, H 4.78, N 8.58. **2a**-Gd: $C_{40}H_{61}Cl_6GdN_8O_{10}P_2Zn$ (1311.27): calcd. C 36.64, H 4.69, N 8.55; found C 36.57, H 4.66, N 8.51. **2a**-Er: $C_{40}H_{61}Cl_6ErN_8O_{10}P_2Zn$ (1321.28): calcd. C 36.36, H 4.65, N 8.48; found C 36.17, H 4.78, N 8.52.

2b-Ln, Ln = La, Nd, Eu, Dy, Er, Lu: Prepared by following the procedure described for compounds **1a**-Ln using **HL**^{2} and (**Vp**)$^{2-}$ as the staring ligands. Crystals of **2b**-La, **2b**-Eu, and powders of **2b**-Nd, **2b**-Dy, **2b**-Er, and **2b**-Lu formed after 5–7 days. Yield: 70–80%. **2b**-La: $C_{41}H_{63}Cl_6LaN_8O_{10}P_2Zn$ (1306.95): calcd. C 37.68, H 4.86, N 8.57; found C 37.55, H 4.90, N 8.50. **2b**-Nd: $C_{41}H_{63}Cl_6N_8NdO_{10}P_2Zn$ (1312.28): calcd. C 37.53, H 4.84, N 8.54; found C 37.48, H 4.82, N 8.49. **2b**-Eu: $C_{41}H_{63}Cl_6EuN_8O_{10}P_2Zn$ (1320.00): calcd. C 37.31, H 4.81, N 8.49; found C 37.27, H 4.78, N 8.47. **2b**-Dy: $C_{41}H_{63}Cl_6DyN_8O_{10}P_2Zn$ (1330.54): calcd. C 37.01, H 4.77, N 8.42; found C 36.89, H 4.80, N 8.39. **2b**-Er: $C_{41}H_{63}Cl_6ErN_8O_{10}P_2Zn$ (1335.30): calcd. C 36.88, H 4.76, N 8.39; found C 36.65, H 4.74, N 8.25. **2b**-Lu: $C_{41}H_{63}Cl_6LuN_8O_{10}P_2Zn$ (1343.01): calcd. C 36.67, H 4.73, N 8.34; found C 36.63, H 4.73, N 8.29.

2c-Ln, Ln = La, Eu, Gd, Er, Lu: Hydrated nitrate $Ln(NO_3)_3\cdot xH_2O$ (0.5 mmol) was dissolved in methanol (2 mL) and mixed with Na**L**^{2} (1 mmol) in methanol (3 mL). The resulting solution was added dropwise with constant stirring to a hot solution of Ni(**Vp**) (0.5 mmol) and heated to reflux for 1 h. The reaction mixture was left in air at room temperature, and crystals of **2c**-La and powders of **2c**-Eu, **2c**-Gd, **2c**-Er, and **2c**-Lu formed after 3–5 days. Yield: 75–85%. **2c**-La: $C_{42}H_{67}Cl_6LaN_8NiO_{11}P_2$ (1332.32): calcd. C 37.86, H 5.07, N 8.41; found C 37.68, H 5.09, N 8.44. **2c**-Eu: $C_{42}H_{67}Cl_6EuN_8NiO_{11}P_2$ (1345.37): calcd. C 37.50, H 5.02, N 8.33; found C 37.53, H 5.05, N 8.36. **2c**-Gd: $C_{42}H_{67}Cl_6GdN_8NiO_{11}P_2$ (1350.66): calcd. C 37.35, H 5.00, N 8.30; found C 37.28, H 4.91, N 8.11. **2c**-Er: $C_{42}H_{67}Cl_6ErN_8NiO_{11}P_2$ (1360.67): calcd. C 37.07, H 4.96, N 8.24; found C 37.12, H 5.08, N 8.19. **2c**-Lu: $C_{42}H_{67}Cl_6LuN_8NiO_{11}P_2$ (1368.38): calcd. C 36.87, H 4.94, N 8.19; found C 36.80, H 4.96, N 8.20.

Supporting Information (see footnote on the first page of this article): IR, ^{1}H and ^{31}P NMR spectral details of the synthesized compounds, molecular structures of **2a**-La and **2b**-Eu, and MS data for **2b**-Nd, **2c**-La, and **2c**-Er.

---

[1] S. Petit, F. Baril-Robert, G. Pilet, C. Reber, D. Luneau, *Dalton Trans.* **2009**, 6809–6815.
[2] A. Pandey, A. Pandey, P. Mayer, W. J. Parak, A. B. Samaddara, *Z. Naturforsch. B* **2009**, *64*, 263–268.
[3] I. Ramade, O. Kahn, Y. Jeannin, F. Robert, *Inorg. Chem.* **1997**, *36*, 930–936.
[4] J. Lisowski, P. Starynowicz, *Inorg. Chem.* **1999**, *38*, 1351–1355.
[5] C. Brewer, G. Brewer, W. R. Scheidt, M. Shang, E. E. Carpenter, *Inorg. Chim. Acta* **2001**, *313*, 65–70.
[6] F. Pointillart, K. Bernot, *Eur. J. Inorg. Chem.* **2010**, 952–964.
[7] G. A. Brewer, E. Sinn, *Inorg. Chem.* **1987**, *26*, 1529–1535.
[8] R. E. P. Winpenny, *Chem. Soc. Rev.* **1998**, *27*, 447–452.
[9] J.-P. Costes, F. Dahan, A. Dupuis, J.-P. Laurent, *New J. Chem.* **1998**, *22*, 1525–1529.
[10] M. Sasaki, K. Manseki, H. Horiuchi, M. Kumagai, M. Sakamoto, H. Sakiyama, Y. Nishida, M. Sakai, Y. Sadaoka, M. Ohba, H. Okawa, *J. Chem. Soc., Dalton Trans.* **2000**, 259–263.
[11] M. Sakamoto, K. Manseki, H. Okawa, *Coord. Chem. Rev.* **2001**, *219–221*, 379–414.
[12] C. Benelli, D. Gatteschi, *Chem. Rev.* **2002**, *102*, 2369–2387.
[13] W. K. Lo, W.-K. Wong, J. Guo, W.-Y. Wong, K.-F. Li, K.-W. Cheah, *Inorg. Chim. Acta* **2004**, *357*, 4510–4521.
[14] W.-K. Lo, W.-K. Wong, W.-Y. Wong, J. Guo, K.-T. Yeung, Y.-K. Cheng, X. Yang, R. A. Jones, *Inorg. Chem.* **2006**, *45*, 9315–9325.
[15] C. E. Burrow, T. J. Burchell, P.-H. Lin, F. Habib, W. Wernsdorfer, R. Clerac, M. Murugesu, *Inorg. Chem.* **2009**, *48*, 8051–8053.
[16] K. O. Znovjyak, O. V. Moroz, V. A. Ovchynnikov, T. Yu. Sliva, S. V. Shishkina, V. M. Amirkhanov, *Polyhedron* **2009**, *28*, 3731–3738.
[17] N. S. Kariaka, V. A. Trush, V. V. Medviediev, T. Y. Sliva, V. M. Amirkhanov, *Acta Crystallogr., Sect. E.* **2013**, *69*, m143.
[18] D. E. Wilcox, *Chem. Rev.* **1996**, *96*, 2435–2458.
[19] R Mitra, M. W. Peters, M. J. Scott, *Dalton Trans.* **2007**, *35*, 3924–3935.
[20] R. A. Mathews, C. S. Rossiter, J. R. Morrow, J. P. Richard, *Dalton Trans.* **2007**, *34*, 3804–3811.
[21] N. H. Williams, B. Takasaki, M. Wall, J. Chin, *Acc. Chem. Res.* **1999**, *32*, 485–493.
[22] L. Bonfa, M. Gatos, F. Mancin, P. Tecilla, U. Tonellato, *Inorg. Chem.* **2003**, *42*, 3943–3949.
[23] B. K. Takasaki, J. Chin, *J. Am. Chem. Soc.* **1993**, *115*, 9337–9338.
[24] B. K. Takasaki, J. Chin, *J. Am. Chem. Soc.* **1995**, *117*, 8582–8585.
[25] R. Breslow, B. Zhang, *J. Am. Chem. Soc.* **1994**, *116*, 7893–7894.
[26] J. Kamitani, J. Sumaoka, H. Asanuma, M. Komiyama, *J. Chem. Soc. Perkin Trans. 2* **1998**, 523–528.
[27] V. V. Skopenko, V. M. Amirkhanov, T. Yu. Sliva, I. S. Vasilchenko, E. L. Anpilova, A. D. Garnovskii, *Usp. Khim.* **2004**, *73*, 797–813.
[28] O. O. Litsis, V. A. Ovchynnikov, S. V. Shishkina, T. Y. Sliva, V. M. Amirkhanov, *Trans. Met. Chem.* **2013**, *38*, 473–479.
[29] K. O. Znovjyak, V. A. Ovchynnikov, T. Yu. Sliva, S. V. Shishkina, V. M. Amirkhanov, *Acta Crystallogr., Sect. E.* **2010**, *66*, m306.
[30] O. V. Amirkhanov, O. V. Moroz, K. O. Znovjyak, E. A. Trush, T. Yu. Sliva, *Acta Crystallogr., Sect. E.* **2010**, *66*, O1102.
[31] V. M. Amirkhanov, V. A. Ovchynnikov, V. A. Trush, V. V. Skopenko, *Zh. Org. Khim.* **1996**, *32*, 376–380.
[32] W.-K. Wong, H. Liang, W.-Y. Wong, Z. Cai, K.-F. Li, K.-W. Cheah, *New J. Chem.* **2002**, *26*, 275–278.
[33] X.-P. Yang, R. A. Jones, Q.-Y. Wu, M. M. Oye, W.-K. Lo, W.-K. Wong, A. L. Holmes, *Polyhedron* **2006**, *25*, 271–278.
[34] J.-P. Costes, G. Novitchi, S. Shova, F. Dahan, B. Donnadieu, J.-P. Tuchagues, *Inorg. Chem.* **2004**, *43*, 7792–7799.
[35] G. Novitchi, S. Shova, A. Caneschi, J.-P. Costes, M. Gdaniec, N. Stanica, *Dalton Trans.* **2004**, 1194–1200.
[36] J.-P. Costes, F. Dahan, W. Wernsdorfer, *Inorg. Chem.* **2006**, *45*, 5–7.
[37] J.-R. Che, Y. Sui, Q.-Y. Luo, R.-Q. Jiang, *Acta Crystallogr., Sect. E: Struct. Rep. Online* **2007**, *63*, m2091–m2092.
[38] Y. Sui, J.-H. Zhang, R.-H. Hu, L.-Y. Yi, *Acta Crystallogr., Sect. E: Struct. Rep. Online* **2007**, *63*, m2089–m2090.
[39] Y. Sui, X.-N. Fang, P. Hu, J. Lin, *Acta Crystallogr., Sect. E: Struct. Rep. Online* **2007**, *63*, m2135–m2136.

[40] L. Guggenberger, E. Muetterties, *J. Am. Chem. Soc.* **1976**, *98*, 7221–7225.
[41] D. Cunningham, J. F. Gallagher, T. Higgins, P. McArdle, J. McGinley, M. O'Gara, *J. Chem. Soc., Dalton Trans.* **1993**, 2183–2190.
[42] J.-P. Costes, F. Dahan, A. Dupuis, J.-P. Laurent, *Inorg. Chem.* **1997**, *36*, 4284–4286.
[43] R. Gheorghe, M. Andruh, J.-P. Costes, B. Donnadieu, M. Schmidtmann, A. Müller, *Inorg. Chim. Acta* **2007**, *360*, 4044–4050.
[44] F. Liu, F. Zhang, *Acta Crystallogr., Sect. E.* **2008**, *64*, m589.
[45] Y.-A. Xiao, X.-K. Fu, Y. Sui, Q. Wu, S.-H. Xiong, *Acta Crystallogr., Sect. E.* **2008**, *64*, m806–m807.
[46] H. Arora, S. K. Barman, F. Lloret, R. Mukherjee, *Inorg. Chem.* **2012**, *51*, 5539–5553.
[47] A. M. Ramadan, J. M. C. Sala, T. N. Parac-Vogt, *Dalton Trans.* **2011**, *40*, 1230–1232.
[48] X. Wu, H. Lin, J. Shao, H. Lin, *J. Mol. Catal. A* **2008**, *293*, 79–85.
[49] A.-M. Fanning, S. E. Plush, T. Gunnlaugsson, *Chem. Commun.* **2006**, 3791–3793.
[50] C. Liu, M. Wang, T. Zhang, H. Sun, *Coord. Chem. Rev.* **2004**, *248*, 147–168.
[51] L. V. Penkova, A. Maciag, E. V. Rybak-Akimova, M. Haukka, V. A. Pavlenko, T. S. Iskenderov, H. Kozłowski, F. Meyer, I. O. Fritsky, *Inorg. Chem.* **2009**, *48*, 6960–6971.
[52] G. M. Sheldrick, *Acta Crystallogr., Sect. A: Found. Crystallogr.* **2008**, *64*, 112–122.
[53] F. Lam, J.-X. Xu, K. S. Chan, *J. Org. Chem.* **1996**, *61*, 8414–8418.
[54] P. G. Lacroix, S. D. Bella, I. Ledoux, *Chem. Mater.* **1996**, *8*, 541–545.

Received: March 25, 2014